



**CHALMERS**  
UNIVERSITY OF TECHNOLOGY

## **Integration of sorbent-based direct air capture into combined heat and power plants with post-combustion carbon capture**

Downloaded from: <https://research.chalmers.se>, 2025-06-01 15:06 UTC

Citation for the original published paper (version of record):

Hoseinpoori, S., Roshan Kumar, T., Beiron, J. et al (2025). Integration of sorbent-based direct air capture into combined heat and power plants with post-combustion carbon capture. *Energy*, 328. <http://dx.doi.org/10.1016/j.energy.2025.136509>

N.B. When citing this work, cite the original published paper.



# Integration of sorbent-based direct air capture into combined heat and power plants with post-combustion carbon capture

Sina Hoseinpoori<sup>a,\*</sup>, Tharun Roshan Kumar<sup>a</sup>, Johanna Beiron<sup>a</sup>, Filip Johnsson<sup>a</sup>,  
Elin Svensson<sup>a,b</sup>, David Pallarès<sup>a</sup>

<sup>a</sup> Division of Energy Technology, Chalmers University of Technology, SE-412 96, Gothenburg, Sweden

<sup>b</sup> CIT Renergy AB, Sven Hultins plats 1, SE-412 58, Gothenburg, Sweden

## ARTICLE INFO

### Keywords:

Direct air capture  
Carbon capture and storage  
Combined heat and power  
District heating  
Process integration  
Optimization  
Techno-economics

## ABSTRACT

Combined heat and power (CHP) plants that provide district heating are underutilized due to seasonal variations in heat demand. This work provides an assessment of the techno-economic potential of integrating sorbent-based direct air capture (s-DAC) into CHP plants in district heating systems, so as to expand the business portfolio of the plant and increase its utilization. The proposed integrated system utilizes the existing CHP infrastructure to provide heat at 100 °C, and high-temperature heat pumps to upgrade available waste heat from a post-combustion carbon capture (PCC) unit, so as to drive a s-DAC process. A bottom-up framework methodology is used to quantify the carbon dioxide removal (CDR) potential of the proposed system and identify the optimal design and operation, while considering cost optimization with respect to fuel type, district heating demand, the extent of heat recovery within the plant, heat and electricity prices, and carbon removal prices.

The results show that for a 167-MW reference plant with PCC, integration of a s-DAC process that is dimensioned for maximum removal (i.e., not optimizing the economics but instead prioritizing the extent of carbon removal) provides additional carbon removal from the atmosphere of 162.7 ktCO<sub>2</sub>/y. A net-positive cash flow is attained at CDR credit prices in the range of 279–685 €/tCO<sub>2</sub> (reflecting zero heat recovery to full heat recovery). For profit-driven operations, the results indicate that for a CDR credit price of 615 €/tCO<sub>2</sub>, s-DAC and PCC contribute 11.8 % and 67.1 %, respectively, of the total yearly net cash flow of the plant.

## 1. Introduction

Carbon dioxide removal (CDR) is expected to play a major role in meeting climate targets by compensating for hard-to-abate emissions [1]. In addition, in the longer run, it will contribute to net-negative emissions due to a likely overshoot in emissions. The European Commission has set the target of reaching net-zero emissions by Year 2050 for the Member States [2]. Some countries, such as Sweden, have set more-ambitious goals and are aiming to achieve net-zero CO<sub>2</sub> emissions by Year 2045 [3]. In this regard, the Government of Sweden estimates that net CO<sub>2</sub> removal in the range of 3–10 MtCO<sub>2</sub>/y in Year 2045 will be required for the country to be achieve the net-zero goal [4].

Several methods have been proposed for CDR, among which biomass combustion with carbon capture and storage (bio-CCS) and direct air capture (DAC) show the highest potentials for large-scale deployment [5]. In this regard, existing biomass-fired, combined heat and power

(CHP) plants provide an opportunity for bio-CCS through investments in end-of-pipe CO<sub>2</sub> capture technologies [6]. Implementing bio-CCS at CHP plants that are currently operating in district heating (DH) systems is expected to be cost-intensive [7], since these plants typically have a relatively low number of equivalent full-load hours, due to the seasonal variations on the heat demand side.

Regarding DAC, temperature vacuum swing adsorption DAC (commonly referred to as solid sorbent DAC, s-DAC) can capture CO<sub>2</sub> from atmospheric air using electricity and low-temperature heat (80–120 °C). While the main contributor to the cost of CDR via s-DAC is currently capital investments, the deployment of s-DAC is also limited by high requirements for energy, mainly in the form of heat [5]. Consequently, the literature on s-DAC often considers cases in which waste heat from industries is used as a heat source [8]. Furthermore, waste heat from industries is considered to be burden-free [9], which increases the carbon removal efficiency of the s-DAC by reducing the amount of

This article is part of a special issue entitled: ECOS2024 published in Energy.

\* Corresponding author.

E-mail address: [sinaho@chalmers.se](mailto:sinaho@chalmers.se) (S. Hoseinpoori).

<https://doi.org/10.1016/j.energy.2025.136509>

Received 20 December 2024; Received in revised form 22 April 2025; Accepted 8 May 2025

Available online 9 May 2025

0360-5442/© 2025 The Authors. Published by Elsevier Ltd. This is an open access article under the CC BY license (<http://creativecommons.org/licenses/by/4.0/>).

CO<sub>2</sub> emitted from powering the CDR process [10]. Given the availability of low-grade (50°–90 °C) waste heat from CHP plants that have been retrofitted with post-combustion capture (PCC) units and the likelihood of future access to a CO<sub>2</sub> transport infrastructure, the co-location and integration of the s-DAC technology at bio-CCS plants in DH systems could be a suitable strategy for achieving large-scale CDR at a relatively low cost, as compared with standalone s-DAC.

The integration of s-DAC into other processes has two main driving forces: 1) to utilize the CO<sub>2</sub> captured; and 2) to utilize clean/waste energy from another process to drive the DAC. Regarding DAC with CO<sub>2</sub> utilization, the usual layout involves an electrolyzer using the by-produced water by DAC to produce hydrogen (which is why the s-DAC technology was originally developed). In this context, Drechler et al. [11] and Jeong-Potter et al. [12] have analyzed the properties of s-DAC integrated with power-to-gas processes. The former proved that the integration of DAC and methanation integration can produce methane from air and hydrogen autothermally while the latter proved the feasibility of using dual functional material for DAC and methanation. Schäppi et al. [13] have integrated s-DAC with a solar-driven redox reactor to produce jet fuel from air which resulted in cost of jet fuel in range 1.2–2€/lit with optimistic values assumed for the cost of DAC. The access to clean energy has also driven the integration of s-DAC with variable renewable energy systems [14] or industrial processes that have waste heat available, in order to increase the overall carbon capture efficiency of the s-DAC. Following this pathway, Bertoni et al. [15] assessed the net removal cost of CO<sub>2</sub> for conceptual integration of s-DAC into a small modular reactor yielding costs slightly higher than those of s-DAC integrated with geothermal or waste heat. Wiegner et al. [16] have investigated the operation of s-DAC integrated with an electricity grid which included a high share of variable renewable electricity to show that the performance of the DAC can improve if the process can adjust to weather changes over time and remove CO<sub>2</sub> flexibly. Leonzio and Shah [17] investigated how s-DAC can be integrated with heat pumps to electrify the technology and concluded that the cost of CDR via DAC can be reduced up to 39\$/tCO<sub>2</sub> compared to stand alone DAC. In addition, some studies have focused on integrating s-DAC with the biomass combustion process. For example, Sagues et al. [18] have investigated the leveled cost of CO<sub>2</sub> removal for integrated bioenergy with CCS plant with s-DAC where s-DAC unit is also responsible for capturing CO<sub>2</sub> from atmosphere. Furthermore, Al-Ansari et al. [19] have examined the integration of s-DAC technologies into a biomass-integrated gasification combined cycle with a CCS unit, in which biomass is combusted exclusively for the provision of energy for s-DAC, so as to maximize the potential for carbon removal. Both of the latter studies have reported improved cost-effectiveness for CO<sub>2</sub> removal when bioenergy with CCS is integrated with s-DAC. Finally, Cheng et al. [20] modeled the optimized integration of s-DAC with NGCC, whereby s-DAC uses steam and electricity from the NGCC, concluding that a CO<sub>2</sub> price in the range of 150–225 \$/tCO<sub>2</sub> is required for a positive net present value (NPV). However, in all cases, the heat used by DAC is not utilized further, i.e. is released to the surrounding ambient-temperature environment. Further, the value and possible utilization of this released heat has not yet been thoroughly investigated. One possible use for the released heat could be from integration of DAC with district heating systems, which are a key component in some energy systems, e.g. in the Nordics. There, while combined heat and power plants currently serve as the primary heat source, a transition toward using heat pumps [22] as main heat suppliers is expected. This shift could significantly reduce the business opportunities available for CHP plants.

This work aims to assess the carbon dioxide removal (CDR) potential of plants integrating combined heat and power, post-combustion capture and direct air capture (here called CHP-PCC-DAC). The specific objectives are to contribute to:

1. Evaluate the potential for DAC as a new business opportunity for CHP plants;

2. Identify the key parameters influencing the performance of the integrated system;
3. Investigate the optimal sizing of the DAC units in such integrated systems and the pricing of CDR credits (a certificate that declares the owner has removed one unit mass of CO<sub>2</sub> removed from atmosphere) required to ensure economic viability under various scenarios; and
4. Analyze the cost-optimal dispatch of the integrated system, including carbon-negative electricity, district heating, and carbon removal credits.

To achieve this, a generalized framework is developed that incorporates process integration with closures of the heat balances, cash flow analysis, and cost-optimization modeling of CHP plant integrated with s-DAC.

## 2. The proposed system

This section describes the proposed CHP-PCC-DAC system, where the term CHP-PCC denotes a combined heat and power (CHP) plant that is equipped with post-combustion CO<sub>2</sub> capture and conditioning<sup>1</sup> (PCC) units, to which a s-DAC process is integrated. All the process equipment considered in the proposed system is technically mature, except for the s-DAC technology [21]. This work considers a generalized CHP plant that delivers DH, electricity, and CDR credit output. Two types of CHP plants are considered: biomass-fired and waste-fired. The difference between these plants is that waste incineration plants primarily serve as a waste management system that operates throughout the year (>8000 h/y), emitting both fossil and biogenic CO<sub>2</sub> (~48 % and 52 %, respectively [7]), while biomass-fired CHP plants, fired with forestry residues, provide carbon-neutral DH and electricity but operate on the basis of adapting the load to the heat-demand, resulting in a yearly utilization factor typically around 50 % [22]. The inability of waste-fired plants to adapt their load to the heat demand curve results typically in that the selling price of the district heating produced is substantially lower than that of the more adaptive biomass-fired plants.

Fig. 1 illustrates the CHP-PCC-DAC system with its main energy flows. The main energy flows that are used to control the operation of the system in the model are marked with the valves. This system, which expands upon the CHP-PCC system described in previous work by some of the authors [23] includes four units besides the CHP plant: post-combustion CO<sub>2</sub> capture and conditioning units (PCC); low-temperature heat pumps (LTHP); high-temperature heat pumps (HTHP); and the s-DAC unit. In the CHP-PCC system, the DH return water (at 50 °C) is heated in a series of heat exchangers from the flue gas and turbine condensers to meet the DH supply temperature, which typically lies in the range of 70°–120 °C [24]. The s-DAC system typically requires a heating medium at 80°–100 °C, depending on its operating conditions [25]. The integration of the s-DAC system into the CHP-PCC system, as shown in Fig. 1, offers the possibility to utilize its electricity and heat with zero-carbon footprint (DH water) at temperatures that are suitable for the s-DAC system. In the proposed system, assuming a DH supply temperature of 90 °C and a minimum temperature difference of 10 °C in the adsorbent bed (as reported in Ref. [26]), the DH water is heated to 100 °C before it enters the s-DAC system.

Based on Roshan Kumar et al. [23], the proposed CHP-PCC-DAC system includes heat pumps to upgrade the recoverable excess heat from the PCC units, thereby increasing the DH output. The recoverable excess heat from the PCC units, designated as low-grade heat (30°–50 °C) and high-grade heat (50°–90 °C), is recovered as warm water at 50 °C and hot water at 90 °C, respectively. The warm water is then upgraded in the LTHP to the DH supply temperature (90 °C), which can either be directed to the HTHP or supplied as DH water. The proposed system includes HTHP, which upgrades the hot water from the

<sup>1</sup> CO<sub>2</sub> compression and liquefaction for transportation by ship.

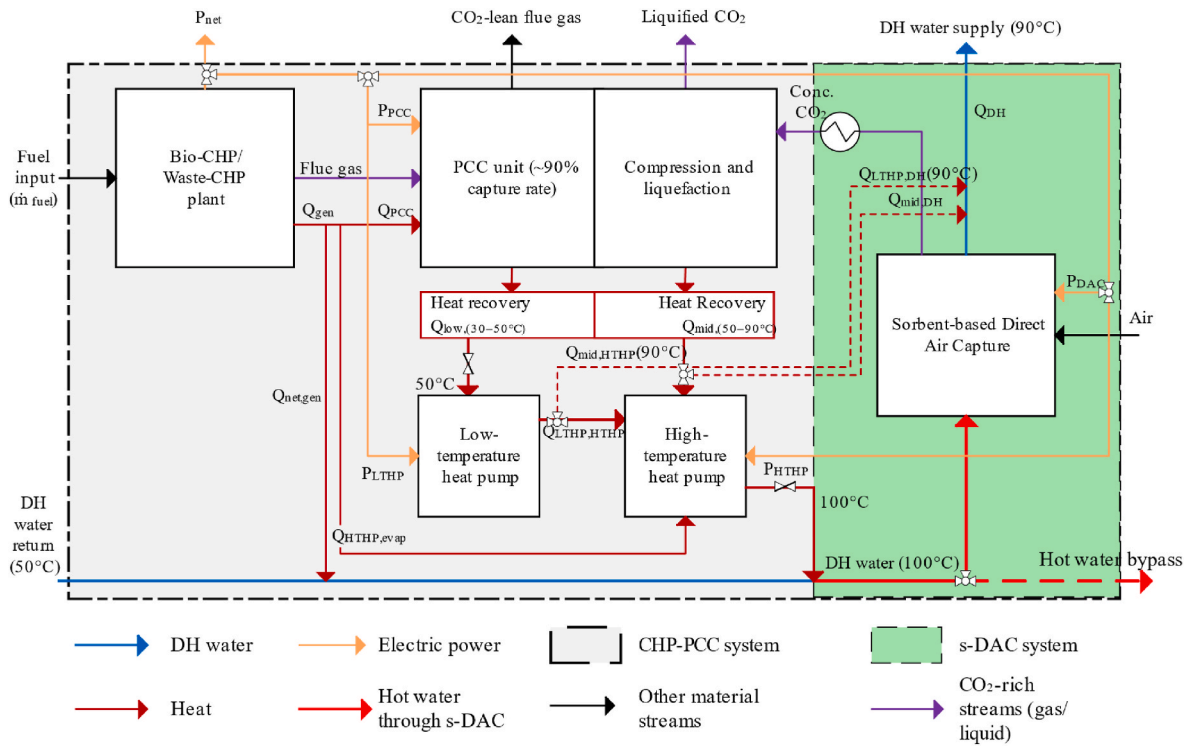


Fig. 1. Schematic of the proposed CHP-PCC-DAC system.

PCC units and LTHP to the target inlet temperature of the s-DAC system (100 °C). It is assumed that LTHP has access to abundant ambient heat as the heat source for the working fluid, whereas HTHP uses low-pressure bleed steam from the CHP plant as its heat source. Furthermore, a minimum temperature difference of 10 °C is assumed in the heat exchangers of the heat pumps, which results in temperature lifts of 80 °C and 20 °C in the LTHP and HTHP, respectively.

The proposed system differs from s-DAC plant integrated with heat pumps is that the proposed system utilizes hot water from the CHP plant and the upgraded excess heat from the PCC unit (at ~100 °C). In contrast, standalone s-DAC systems typically rely on geothermal heat (limited to specific locations [8]), industrial waste heat (subject to site-specific constraints [8]) or heat from air-source heat pumps (the performance of which is affected by variations in the outdoor temperature [27]). Furthermore, the difference in the heat source temperatures and the resulting temperature lift in the heat pumps directly affect the electricity requirements of the s-DAC system. In addition, the proposed system benefits from existing access to large volumes of water and the associated water supply systems at the CHP plant. In contrast, integration of s-DAC systems at industrial sites could be limited by water availability, necessitating additional investments in heat recovery and water supply systems.

### 3. Methodology

Fig. 2 illustrates the framework used in this work for process integration and techno-economic optimization of the proposed CHP-PCC-DAC system. First, steady-state process models and process integration methods are used to evaluate the impact that integrating PCC and s-DAC units has on the performance of the CHP plant (Section 3.1). Next, a feasibility assessment and cash-flow analysis are conducted to assess the CDR potential and the economic feasibility of the proposed system for different levels of heat recovery from the PCC units (Section 3.2), which are then used as inputs to a linear investment and dispatch optimization model (Section 3.3). The model simultaneously optimizes the installed capacities of the heat pumps and s-DAC system, along with the dispatch

of the integrated CHP-PCC-DAC plant, to maximize the annual net cash flow (NCF). The optimization is subject to electricity prices, heat and CDR credits prices (The value that CDR credits are purchased at voluntary markets), and investment costs.

Carbon dioxide transportation and long-term storage costs are highly dependent upon the chosen transport mode and transport distance. Based on the work of Karlsson et al. [28], transportation costs for industries in Sweden are in the range of 10–50 €/tCO<sub>2</sub>. In this work, to ensure a conservative estimate CDR prices, include the estimated cost of CO<sub>2</sub> capture and liquefaction onsite (via bio-CCS or s-DAC) along with the upper-bound transportation and storage costs for Sweden i.e. the above mentioned transport cost of 50 €/tCO<sub>2</sub> is considered together with a long-term storage cost of 15 €/tCO<sub>2</sub> based on the offshore sequestration case described by Mühlbauer et al. [29].

#### 3.1. Process integration

Table 1 summarizes the process data and assumptions made for the s-DAC and heat pumps of the proposed system. The PCC unit is an amine absorption unit which uses 30 %wt Monoethanolamine (MEA) solution as solvent [30]. The process uses an absorber filled with wetted packing for contacting flue gas and solvent and a stripper to regenerate the solvent. A water washing section is also considered to limit MEA slip to environment. The process design has been adapted from Roshan Kumar et al. [23] where the main model parameters are detailed. The recoverable excess heat from the PCC units is estimated from the actual cooling load curve (ACL), as described in Ref. [23]. Note that the ACL derived from that work [23] is applicable to biomass-fired CHP plants. To simplify the heat integration in the present work, it was assumed that the differences in heat recovery potential due to different flue gas compositions would be negligible. The LTHP operates with a temperature lift of 80 °C, with a working fluid temperature that ranges from 20 °C to 100 °C, whereas the HTHP operates with a temperature lift of 20 °C, with a working fluid temperature that ranges from 90 °C to 110 °C. These temperature levels were used to estimate the coefficient of performance (COP) of a reversible Carnot heat pump, from which the

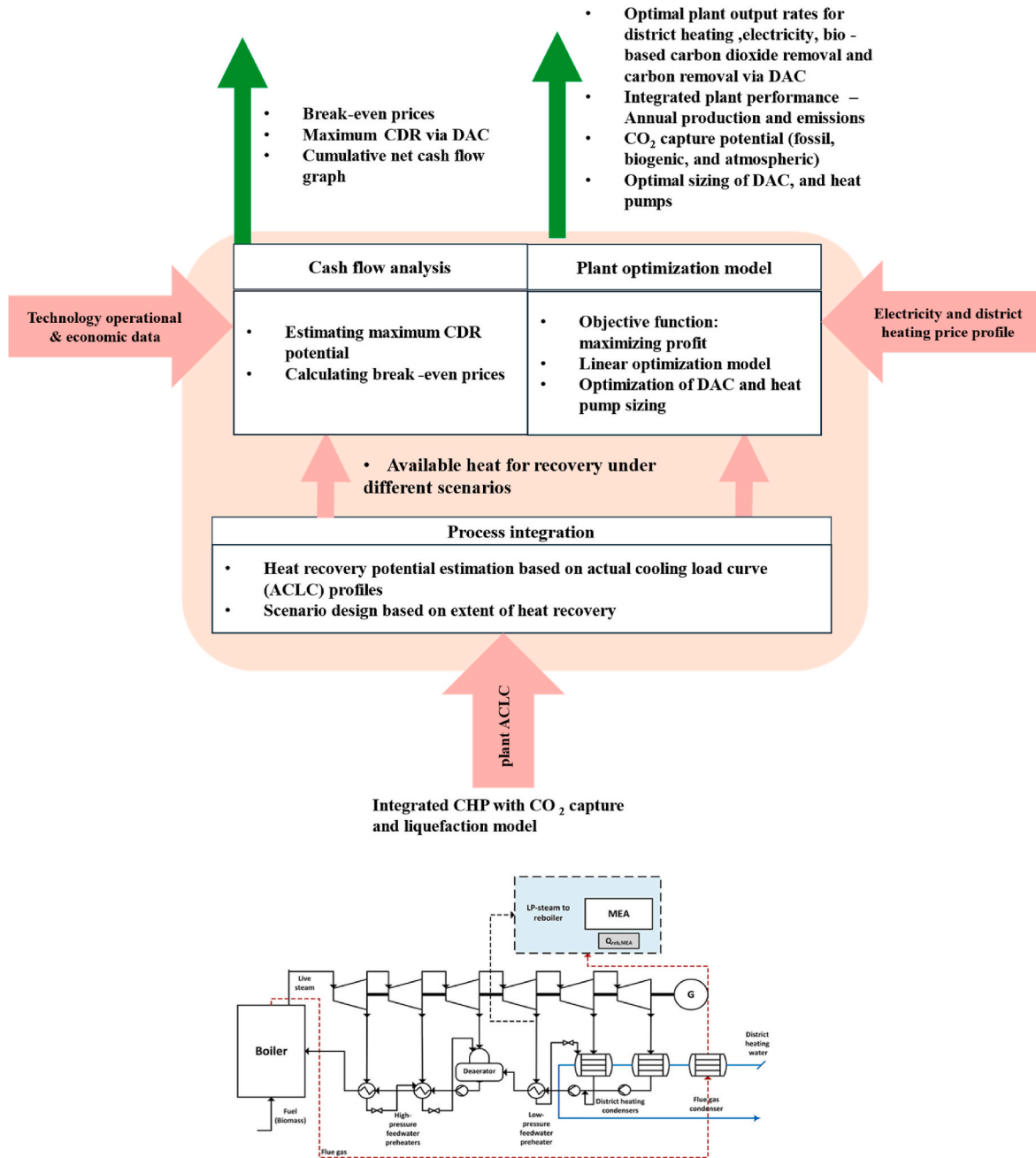


Fig. 2. Overview of the framework used in this work. The red-shaded and green-shaded boxes indicate the input data and outputs, respectively.

COP of the heat pumps was estimated using an assumed Carnot efficiency of 45 %. Assuming a minimum temperature difference of 10 °C in the heat exchangers of the heat pump, the LTHP and HTHP were sized based on the heat demands in their respective condensers ( $Q_{cond,HP}$ ), as expressed in Eq. (1). The electric power demand and evaporator loads ( $Q_{evap}$ ) of the heat pumps were calculated as shown in Eq. (2) and Eq. (3), respectively.

$$Q_{cond,HP} = (\dot{m}_{sink} * C_p * (T_{sink,target} - T_{sink,supply})) \quad (1)$$

$$P_{HP} = Q_{cond,HP} / \left( \eta_{Carnot} * \left( 1 - \frac{T_{cond}}{(T_{wf\_cond} - T_{wf\_evap})} \right) \right) \quad (2)$$

$$Q_{evap,HP} = Q_{cond,HP} - P_{HP} \quad (3)$$

The extent of heat recovery from the PCC unit is expected to impact

the results, as it directly influences the level of available heat to drive the s-DAC unit and, thereby, the amount of CDR attainable via s-DAC. Therefore, three scenarios are considered for heat recovery from the PCC unit (see Fig. 1):

1. No heat recovery
2. *Mid-level heat recovery*: Recovery of excess heat at temperatures between 50 °C and 90 °C through heat exchangers
3. *Full heat recovery*: Recovery of excess heat at temperatures between 50 °C and 90 °C through heat exchangers and at temperatures between 30 °C and 50 °C through LTHP

### 3.2. Cash flow analysis

To assess the economic profitability of the proposed system, a cash flow analysis was conducted for two retrofit cases: i) departing from a

**Table 1**

Summary of the s-DAC, PCC, and heat pump data and assumptions used in this work.

		Comment/References
<b>s-DAC</b>		
Electricity requirement	500 kWh/tCO <sub>2</sub>	Long-term estimates for Climeworks s-DAC technology [8]
Heat requirement	1500 kWh/tCO <sub>2</sub>	
Minimum temperature difference $\Delta T_{\min}$ between the adsorbent bed and heating medium	10 °C	[31]
Liquid CO <sub>2</sub> specifications	16 bar, -26.5 °C	Adopted from the Northern Lights project [32]
<b>CO<sub>2</sub> capture and conditioning units</b>		
CO <sub>2</sub> capture rate (90 %)	90	Constant design parameter
Lean solvent composition (wt.% MEA in H <sub>2</sub> O)	30	Benchmark monoethanolamine (MEA) solvent.
Minimum temperature difference in heat exchangers and stripper reboiler (°C)	10, 5	Assumed
Recoverable heat between 50 and 90 °C (MJ/kgCO <sub>2</sub> )	0.58	Estimated from ACLC in Ref. [33] for recoverable heat between 47–86 °C and 30–47 °C, respectively.
Recoverable heat between 30 and 50 °C (MJ/kgCO <sub>2</sub> )	0.61	
<b>Heat pumps (LT &amp; HT)</b>		
Temperature lift	LTHP 80 °C HTHP 20 °C	Estimated assuming a minimum temperature difference of 10 °C in the heat exchangers of the heat pumps
Heat sink	LTHP 50°–90 °C HTHP 90°–100 °C	Warm water supply and target temperatures through the LTHP condenser. Hot water supply and target temperatures through the HTHP condenser
Heat source	LTHP 30 °C HTHP 100 °C	Ambient temperatures + $\Delta T_{\min}$ Low-pressure steam (1.03 bar) extracted from the turbine
Carnot efficiency	0.45	Assumption

CHP plant already equipped with PCC an investment is made to integrate s-DAC; and ii) departing from an existing CHP plant not equipped with PCC, an investment is made to integrate both s-DAC and PCC. For each of the retrofit alternatives (implementation of the CHP-PCC-DAC system departing from CHP or from CHP-PCC), the analysis considered a retrofit perspective, i.e., the investment and operational costs of the units added are paid with the incremental revenue streams (CDR credits) generated from the same units. Obviously, if the added units consume heat and power that represented income before the retrofit, these decreased sales were considered as costs associated with the retrofit. With this, change the net annual cash flow (NCF) is expressed as:

$$NCF = \sum_{t=1}^{8760} \left[ C_{neg} * \Delta \dot{m}_{CDR}(t) + C_{EU-ETS} * \Delta \dot{m}_{CO_2, fossil}(t) - C_{DH}(t) * \Delta Q_{DH} - C_P(t) * \Delta P_{net} - C_{fuel} * \Delta \dot{m}_{fuel}(t) - \sum_{units} fixed\ Opex_{units} \right] - \sum_{units} (C_{unit}^{inv} * S_{unit}) / ANF \quad (4)$$

Setting the change in the net annual cash flow equal to zero and solving for  $C_{neg}$  provides the break-even values of the CDR credit price, i.e. the price making the retrofit economically neutral.

### 3.3. Plant optimization model

A linear optimization model was developed to determine the profit-optimal plant dispatch and sizing of the heat pumps and s-DAC sections for the proposed CHP-PCC-DAC system. This optimization consists of maximizing the objective function expressing the increase in the annual net cash flow of the system [Eq. (4)], which comprises revenues from selling electricity, DH, CDR credits (from capture of both biogenic and atmospheric CO<sub>2</sub>), and avoided CO<sub>2</sub> tax (due to capturing the fossil share of the fuel), while accounting for the costs related to fuel and investments in new equipment. The optimization provides as output the retrofit sizing and plant operation which yields a maximization of the net annual ash flow (Eq. (4)).

The overall heat and power generation in the CHP is calculated according to:

$$Q_{gen}(t) = \dot{m}_{fuel}(t) * LHV * \eta_{Q, CHP} \quad (5a)$$

$$P_{gen}(t) = \dot{m}_{fuel}(t) * LHV_{fuel} * \eta_{P, CHP} \quad (5b)$$

where the fuel feeding rate is constrained by the boiler capacity, such that:

$$\dot{m}_{fuel} * LHV_{fuel} \leq Cap_{Boiler} \quad (6)$$

It should be noted that the optimization model assumes constant heat and electricity efficiency for the CHP plant independent of the load level.

The resulting net power output,  $P_{net, gen}$ , is calculated from the balance between the power generated and that linked to internal plant consumption:

$$P_{gen}(t) = P_{net, gen}(t) + P_{PCC}(t) + P_{DAC}(t) + P_{HTHP}(t) + P_{LTHP}(t) \quad (7)$$

The heat extracted from the steam cycle is used to satisfy the heat demand, driving the PCC unit, and providing heat to the heat pumps (see Fig. 1). A heat equal to 17.5 % of the total energy value of the fuel combusted is added to the net heat generation of the CHP plant due to flue gas condensers ( $Q_{FGC}$ ). The constant percentage is assessed based on the steady state model for the plant.

$$Q_{net, CHP}(t) = Q_{gen}(t) - Q_{PCC}(t) - Q_{HTHP, evap}(t) + Q_{FGC}(t) \quad (8)$$

The total amount of CDR credit to be sold at CO<sub>2</sub> price,  $C_{CDR}$ , consists of the sum of the biogenic CO<sub>2</sub> captured from fuel combustion,  $m_{CDR, bio}$ , and the atmospheric CO<sub>2</sub> captured via s-DAC,  $m_{CO_2, DAC}$ . The CDR attained via the PCC unit depends on the biogenic share of the fuel, such that:

$$\dot{m}_{CDR, PCC}(t) = \dot{m}_{CO_2, PCC}(t) * BS \quad (9)$$

where the total amount of CO<sub>2</sub> captured via PCC, ( $\dot{m}_{CO_2, PCC}$ ), is calculated based on the fuel feeding rate, its carbon content (CC), and the constant capture rate (CR) to capture 90 % of the generated CO<sub>2</sub>:

$$\dot{m}_{CO_2, PCC}(t) = \dot{m}_{fuel}(t) * CC * CR * \frac{M_{CO_2}}{M_c} \quad (10)$$

Note that the fossil emissions captured via PCC are added to the objective function for optimization [Eq. (4)] in the form of avoided CO<sub>2</sub> tax. The heat and electricity requirements of the PCC unit are calculated based on the mass flow of captured CO<sub>2</sub> ( $\dot{m}_{CCS}$ ), as follows:

$$Q_{PCC}(t) = \dot{m}_{CO_2, PCC}(t) * Q_{CCS} \quad (11)$$

**Table 2**  
Initial parameters for assessing the net cash flow of the CHP plant before retrofit.

Parameters	Description	Comments/References
$Cap_B$	Boiler capacity	167 MW based on Västerås Unit 6, Västerås, Sweden
$C_p$	Price of electricity	Hourly time series for southern Sweden (SE3) in Year 2022 (average of 129 €/MWh)
$C_{DH}$	Price of DH	Monthly averages for a network in southern Sweden (year average of 10.26 €/MWh)
$C_{fuel}$	Fuel price	26.2 €/MWh (biomass), -7.7 €/MWh (waste) [35]
CC	Fuel carbon content on weight basis	33.9 wt% for waste and 33.5 wt% for biomass [36]
BS	Biogenic share of the fuel carbon content	100 % and 52 % for biomass and waste, respectively [6,7]
LHV	Fuel Lower heating value	11.37 MJ/kg (biomass), 12.13 MJ/kg (waste) [36]
$\eta_{Q,CHP}$	CHP heat efficiency, LHV basis	71.3 %
$\eta_{p,CHP}$	CHP electric efficiency, LHV basis	24.6 %

$$P_{PCC,tot}(t) = \dot{m}_{CO_2,PCC}(t) * (P_{PCC} + P_{C\&L}) \quad (12)$$

The operation of the s-DAC is driven by electricity from the CHP plant and available heat, with the latter representing a constraint, given that it is limited by the energy available in the hot water at the s-DAC inlet. This available heat is expressed as the sum of the HTHP output and the net heat output of the CHP plant after PCC:

$$Q_{DAC}(t) \leq (Q_{net,CHP}(t) + Q_{out,HTHP}(t)) * \frac{\Delta T_{DAC}}{T_{DH,in} - T_{DH,out}} \quad (13)$$

where the heat output of the HTHP is comprised of three parts: mid-level heat recovered and sent to the HTHP ( $Q_{mid,HTHP}$ ), the part of the LTHP heat output that is upgraded via the HTHP ( $Q_{LTHP,HTHP}$ ),

and the heat produced by the HTHP ( $Q_{HTHP}$ ):

$$Q_{out,HTHP}(t) = Q_{LTHP,HTHP}(t) + Q_{mid,HTHP}(t) + Q_{HTHP}(t) \quad (14)$$

with the heat production required from HTHP being determined based on temperature differences:

$$Q_{HTHP}(t) = Q_{LTHP,HTHP}(t) * \frac{\Delta T_{HTHP}}{\Delta T_{LTHP}} + Q_{mid,HTHP}(t) * \frac{\Delta T_{HTHP}}{\Delta T_{Hx}} \quad (15)$$

The heat provided to the DH network,  $Q_{DH}(h)$ , is calculated as the sum of the heat that is directly extracted from the CHP plant, the  $Q_{net,CHP}$ , the  $Q_{LTHP,DH}$ , the  $Q_{mid,DH}$  and the  $Q_{HTHP}$  (see Fig. 1), as expressed by Eq. (16). It should be noted that all the cases considered with carbon capture lead to a reduced heat supply from the CHP plant to the DH network, as compared with the case without PCC. That is, with heat extraction to drive the PCC, the CHP plant is not able to provide the same amount of heat after PCC and integration as before their integration. Still, the heat output profile of the reference CHP plant is used as the heat demand profile for the CHP-PCC-DAC to incentivize the supply of heat.

Moreover, the model assumes a constant heat supply temperature. Thus:

$$Q_{DH}(t) = \min(Q_{DH,dem}(t), Q_{net,CHP}(t) + Q_{LTHP,DH}(t) + Q_{mid,DH}(t) + Q_{HTHP}(t)) \quad (16),$$

**Table 3**  
Sensitivity analysis parameters.

Parameters	Values	Reference/Comment
Heat price	-50 %, +50 %, +100 %, +900 %	Profile in southern Sweden (average, 10.26 €/MWh)
Electricity price value	±30 %	Profile in southern Sweden (SE3) in Year 2022 (average, 129 €/MWh)
Electricity price volatility	Low/High	Low: the predicted electricity price profile in Year 2050 in northern Sweden (SE1) [38] High: the predicted electricity price profile in Year 2050 in southern Sweden (SE4) [38]
Operational hours	Waste-fired CHP: heat profile of waste-fired CHP with 8000 full-load hours/year biomass-fired CHP plant: heat profile of the biomass-fired CHP plant with 4500 full-load hours/year	
Fuel type	Biomass/Municipal solid waste (base case)	
Specific CAPEX (s-DAC)	8, 24, 70 M€/tCO <sub>2</sub> h	24 M€/tCO <sub>2</sub> is the base case. The values represent the current (upper-bound) and future cost (lower-bound) estimates (Young et al., 2023b)

directly to DH ( $Q_{mid,DH}$ ) is determined based on the low-temperature (30°–50 °C) heat recovered from the PCC unit and fed directly to DH ( $Q_{LTHP,DH}$ ):

$$Q_{mid}(t) = Q_{mid,DH}(t) + Q_{mid,HTHP}(t) \quad (17)$$

$$Q_{LTHP}(t) = Q_{LTHP,DH}(t) + Q_{LTHP,HTHP}(t) \quad (18)$$

The s-DAC heat and electricity demands are expressed as:

$$Q_{DAC,tot}(t) = \dot{m}_{CO_2,DAC}(t) * Q_{DAC} \quad (19)$$

$$P_{DAC,tot}(t) = \dot{m}_{CO_2,DAC}(t) * (P_{DAC} + P_{C\&L}) \quad (20)$$

The installed capacity of the s-DAC unit is a float number rather than an integer. Commonly, the installed capacity of the s-DAC is calculated as the capacity per module multiplied by the number of modules. Here, it is assumed that modules can be designed for different capacities.

### 3.4. Case study

The case study was used a reference waste-CHP plant with a thermal input capacity of 167 MW<sub>th</sub> (based on Västerås Unit 6, in the city of Västerås, Sweden, and detailed in Ref. [6]), which is representative of a typical large CHP plant in Sweden [34]. The electricity prices were taken from southern Sweden (price region SE3 during Year 2022, with a yearly average of 129 €/MWh). District heating prices were the average monthly prices that waste CHP receives for supplying heat, and they are taken from a representative municipality, also in southern Sweden, with a yearly average of 10.26 €/MWh [7]. The initial parameters for assessing the net cash flow of the CHP plant before retrofit are presented in Table 2.

To provide insights into the roles of the different parameters, a sensitivity analysis was conducted for the six key parameters listed in Table 3:i) the fuel type, impacting the share of biogenic CO<sub>2</sub> captured, CHP heat and electric efficiencies and, therefore, the availability of heat for s-DAC; ii) the DH demand profile, impacting the operational hours of the plant and, consequently, the return on investment; iii) the heat price,

impacting the cost-effectiveness of the heat pumps in recovering heat from the PCC unit. A large range of heat prices are considered here between -50 % and +100 % with and an additional case of 900 %

The amount of mid-temperature (50°–90 °C) heat recovered and fed

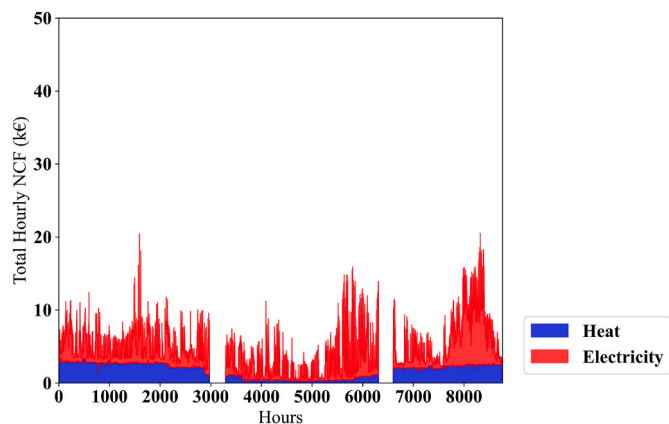


Fig. 3. Hourly NCF levels from heat and electricity sales of the reference CHP plant before PCC and s-DAC integration. Note that the two time periods without production correspond to maintenance shutdowns.

higher price of heat (a value close to consumer prices) is also considered as representative price for load following district heating plants in Sweden. iv) the electricity price; v) electricity price volatility, which impacts the operational cost of producing each of the plant's outputs and characterize different future energy systems (e.g., where greater penetration of variable renewable electricity implies higher price volatility [37]); and vi) the s-DAC-specific CAPEX, which is expected to have a strong impact on the economics of the system while being highly uncertain.

Given the parameters listed in Tables 1 and 2, the calculated hourly NCF, of the reference (i.e., waste-fired) case before the addition of PCC and s-DAC is depicted in Fig. 3. Electricity sales constitute a large share (68.3 %) of the NCF due to the relatively high prices for the electricity used.

#### 4. Results and discussion

First the results with the calculated CO<sub>2</sub> prices that ensure the economic feasibility of the integrated plant with maximized carbon dioxide removal of the CHP-PCC-DAC system is presented for a scenario where the goal is maximized carbon removal rather than economic profit. Thereafter, the results of the economic optimization of the process design and operation are presented, alongside a sensitivity analysis of the six main operational parameters with regards to the amount of carbon dioxide removed.

##### 4.1. Maximised carbon dioxide removal: break-even price of CDR credit

In this subsection, it is assumed that the principle guiding the retrofit is maximized carbon removal via s-DAC rather than optimization of the economic aspect of the retrofit. Thus, the s-DAC module is sized to the maximum available heat at 100 °C for s-DAC, i.e., the sensible heat from DH water temperature ranging from 100 °C to 90 °C (as shown in Fig. 1). Table 4 presents the maximum carbon removal potential via s-DAC for each heat recovery scenario. For the full heat recovery potential, there

Table 4

Maximum atmospheric CDR potential for the different heat recovery scenarios. The corresponding value for biogenic CDR is 162.7 ktCO<sub>2</sub>/y for all the heat recovery scenarios.

	Heat recovery scenario		
	No heat recovery	Mid-level heat recovery	Full heat recovery
Maximum CDR potential via s-DAC (ktCO <sub>2</sub> /y)	74.8	102	158.1

Table 5

Break-even prices of CDR credits required to ensure economic feasibility of the CHP-PCC-DAC system sized for maximum carbon removal.

Breakeven prices (€/tCO <sub>2</sub> )	Heat recovery scenario		
	Retrofit cases	No heat recovery	Mid-level heat recovery
DAC-PCC retrofit of the CHP plant	279	312	405
DAC retrofit of the CHP-PCC plant	620	592	685

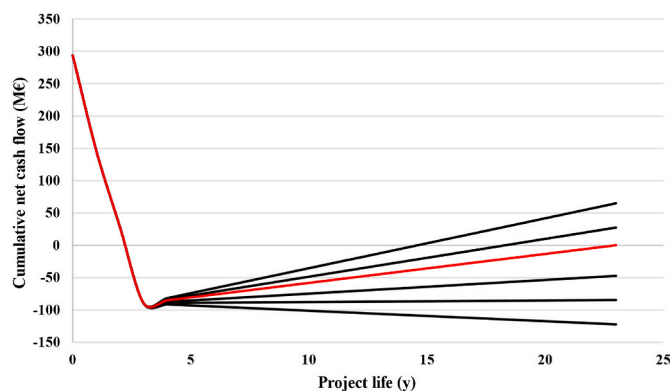


Fig. 4. Cumulative net cash flow over the project lifetime of the proposed CHP-PCC-DAC system for the s-DAC retrofit of the CHP-PCC plant, without heat recovery. The black lines indicate the CDR credit prices. The red curve indicates the break-even CDR.

will be no net electricity generation from the CHP plant, as all of the electricity will be consumed internally, i.e., the system delivers only carbon dioxide removal and DH, and the boiler load follows the heat demand curve. Table 5 presents the break-even prices for CDR credit that would ensure the economic feasibility of the CHP-PCC-DAC system sized for maximum carbon removal.

As presented in Table 5, although the *Full heat recovery* scenario removes more CO<sub>2</sub> from the air (given that the potential for s-DAC is limited by heat availability) and generates higher revenues due to capturing more CO<sub>2</sub> than the *No heat recovery* scenario, it has a higher break-even price than the other two heat recovery scenarios. This is due to the high investment costs for the large LTHPs required for the recovery of heat at temperatures between 30 °C and 50 °C. Furthermore, the break-even CDR prices for the DAC-PCC retrofit of the CHP plant are much lower than those for the s-DAC retrofit of the CHP-PCC plant. This can be explained by the substantial addition of carbon removal from the PCC to the NCF which entails a much lower cost compared to carbon

Table 6

Summary of the economic and technical parameters for the optimization model.

Parameters	Description	Comments/References
C <sub>CDR</sub>	CDR credit price	In the range of 100–1000 €/tCO <sub>2</sub>
C <sub>EU-ETS</sub>	Cost of emitting fossil-based emissions	62 €/tCO <sub>2</sub> , annual average EU-ETS price in Year 2022. Note that this is a conservative value, representing roughly half of Sweden's carbon tax of 132 €/tCO <sub>2</sub> [39]
C <sub>DAC</sub>	Specific investment cost	24 M€/tCO <sub>2</sub> installed capacity [40]
m <sub>sorbent</sub>	Sorbent consumption	7.5 kg/tCO <sub>2</sub> [8]
C <sub>sorbent</sub>	Sorbent price	7000 €/t [40]
Q <sub>HTHP, evap</sub>	Steam bleed as heat source for the evaporator of HTHP model	6.5 MW derived from the Epsilon model
ANF	Annualization factor	9.82, assuming a discount rate of 8 % and a design plant lifetime of 20 years, excluding 3 years for construction.

removal from s-DAC but is still sold at the same CDR price. This increases the overall CDR profit margins and results in a lower break-even CDR price.

Fig. 4 shows the results of the cumulative cash flow analysis for the s-DAC retrofit of the CHP-PCC case, for the *No heat recovery* scenario. The cumulative cash flow is plotted against the designed plant lifetime (from construction to the end of life, here taken as 20 years) for varying CDR credit prices (ranging from 400 €/tCO<sub>2</sub> to 700 €/tCO<sub>2</sub>). For the case plotted, investing in the retrofit will achieve a positive cumulative cash flow for CDR credit prices >620 €/tCO<sub>2</sub> (see also Table 5). Equal values for inflation and discount rates are assumed (which results in linear trends, in contrast to the curves obtained when applying a discount rate that is higher than the inflation rate, which would yield higher break-even CDR credit prices).

#### 4.2. Maximized net cash flow: optimal system sizing and operation

The model was run over one full year of operation with a temporal resolution of 1 h for electricity price, heat price, and heat demand presented in Table 2. The additional specifications of the main parameters in the model required for optimizing the net cash flow of the plant after the retrofit are presented in Table 6.

In this subsection, the system is designed to operate according to the principle of maximized net cash flow. For this, the case in which the CHP-PCC (waste-fired throughout this subsection) is retrofitted with the addition of a s-DAC is in focus. The PCC unit is sized to capture 90 % of the CO<sub>2</sub> in the flue gas, and the s-DAC unit is sized to maximize the NCF. The CDR credit price for the base case is assumed to be 615 €/tCO<sub>2</sub>, which results from summing 550 €/tCO<sub>2</sub> (the maximum value of the cost projected for CDR via s-DAC [26]) and 65 €/tCO<sub>2</sub> (the cost for transportation and sequestration).

The results show that under economically optimal retrofit and operation 110.7 ktCO<sub>2</sub> are removed via s-DAC and 207.2 ktCO<sub>2</sub> via PCC annually. Although s-DAC is responsible for around 35 % of the total carbon removal, it does not have the same share of the NCF from CDR credit sales due to the associated high investment and operational costs.

Fig. 5 shows the load level of the boiler and district heating output for both CHP plant and CHP-PCC-DAC system. As seen, while the reference CHP plant can meet the DH demand by continuously adapting its load, the retrofitted CHP-PCC-DAC system most often does not meet the reference DH demand in a cost-effective way (mainly due to the heat needed to power the PCC unit). Thus, even though the PCC-DAC-retrofitted plant operates at full load for most of the year (as shown in Fig. 5), it delivers 13 % less heat to the DH network compared with the

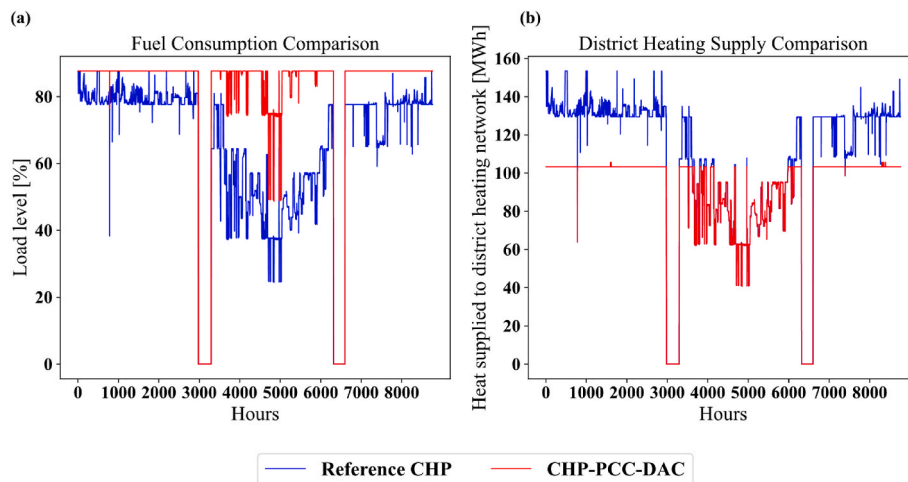


Fig. 5. a) Boiler load levels over the year for the Reference CHP plant and for the CHP-PCC-DAC plant following the DAC-PCC retrofit of the CHP plant. b) Amounts of heat supplied to the district heating network over the year, before (Reference CHP) and after integration of the PCC and s-DAC (CHP-PCC-DAC).

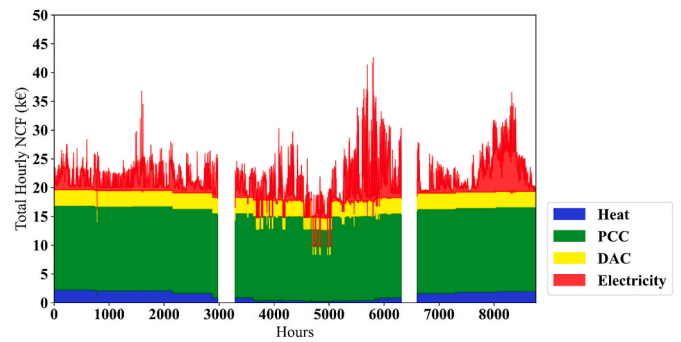


Fig. 6. The shares of optimized hourly NCF for each product from the CHP-PCC-DAC system (base case): CO<sub>2</sub> captured from the flue gas (66.1 %), CDR via s-DAC (12 %), district heating (6.3 %), and electricity (15.4 %).

reference CHP plant. This impacts the utilization rate (i.e., the ratio of full-load equivalent hours in a year to the total hours in a year) of the plant, which increases from 0.73 for the original reference CHP plant to 0.91 for the CHP-PCC-DAC system. From the results regarding the NCF levels of the plant (Fig. 5), integration of PCC into the CHP plant would increase the utilization rate of the CHP-PCC-DAC. However, it also implies that more biogenic carbon is combusted, captured and stored, instead of being used for other purposes.

Fig. 6 shows the time-resolved NCF levels from each product (sales of heat, electricity, and CO<sub>2</sub> captured by PCC and s-DAC). It is evident that although the CHP-PCC-DAC system still operates to provide DH, the main revenue streams are distributed on a yearly basis as according to: CO<sub>2</sub> captured from the flue gas (66.1 %); CO<sub>2</sub> captured through s-DAC (12 %); electricity (15.4 %); and DH (6.3 %). These values are compared to the revenues before the retrofit shown in Fig. 3. It should be noted that the higher NCF share from electricity compared to that from heat is due to the relatively high electricity prices in Year 2022 for southern Sweden (averaging 129 €/MWh). Moreover, it is worth noting in Fig. 6 the red spikes related to momentary peaks in electricity prices. In addition, the weak contribution of DH NCF is due to the relatively lower prices of heat compared to the carbon removal price. This result highlights that the business case for CHP plants might change towards having CDR via capturing biogenic carbon dioxide as the main product in the future, rather than supplying heat and electricity. This may raise concerns regarding the efficient use of biomass, which needs to be addressed at the policy level and is beyond the scope of this work.

For the base case reported in Fig. 6, the utilization rate of the s-DAC system is 90.4 %, while that of the CHP plant is 91.9 %, indicating that

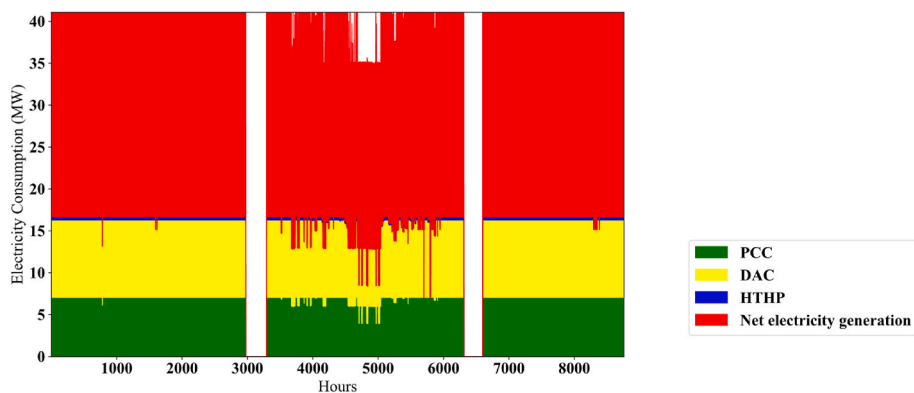


Fig. 7. Consumption shares of the electricity generated in the CHP-PCC-DAC plant for s-DAC (22.1 %), PCC (17.2 %), HTHP (0.7 %), and net electricity generation (60 %).

CDR is the most-valuable product most of the time, except for hours with very high electricity prices (>550 €/MWh).

Fig. 7 shows the following consumption shares of the total electricity generated for the base case: s-DAC (22.1 %), PCC (17.2 %), and HTHP (0.7 %), leaving a share of 60 % available for sale. Thus, the net power output of the CHP-PCC-DAC system is reduced by 37 % compared to the CHP-only case.

The potential for CDR via s-DAC is always limited by the availability of heat in the plant and not by the availability of electricity (as seen from the net electricity sales throughout the year in Fig. 7), as it is not cost-effective for the plant to meet the demand during most of the year. Additionally, it is not allowed to operate at a higher load than that required to meet the district heating (DH) demand.

The results of this work align with conclusions in previous literature on integrating s-DAC and PCC into natural gas combined cycle: an increase in the base load and profit of the plant for scenarios with high CO<sub>2</sub> price [20]. However, the current study reveals further benefits from using the district heating at lower temperatures instead of the steam in power cycles, which results in larger installed capacities of DAC.

At any given time, the amount of heat that is available for recovery depends on the DH demand, since the DH demand determines the fuel consumption rate, which in turn determines the amount of CO<sub>2</sub> that is captured via PCC and, thus, the recoverable excess heat. For the base

case, LTHP is not economically feasible according to the model results, as the revenues from DH deliveries cannot justify the investment and operational costs in the base case. However, the model results suggest recovering the heat available at temperatures in the range of 50°–90 °C (due to the lower specific investment cost for the HTHP that follows from its higher COP: 8.62). Investment in LTHP is shown to be attractive only at lower electricity prices or higher heat prices (<150 €/MWh, which is the price for around 5700 h in the modeled year and a 100 % higher heat price). Under these conditions, larger s-DAC units would be installed (thereby allowing higher rates of CO<sub>2</sub> removal via s-DAC), and the heat output of the plant would increase. Such an increase would compensate for the lower revenue from electricity sales and the high investment costs for LTHP and s-DAC.

### 4.3. Sensitivity analysis: impact on carbon removal

Fig. 8 illustrates the results from the sensitivity analysis of five of the six key parameters; the sixth parameter (s-DAC investment costs) is discussed in the text. Please refer to Table 3 for the list of parameters. Overall, the values for the overall carbon removal potential from the entire system (CHP-PCC-DAC) are in the range of 106–515 ktCO<sub>2</sub>/y. Below, the impacts of the six key parameters are discussed.

The operation of the boiler at 8000 full-load hours per year results in

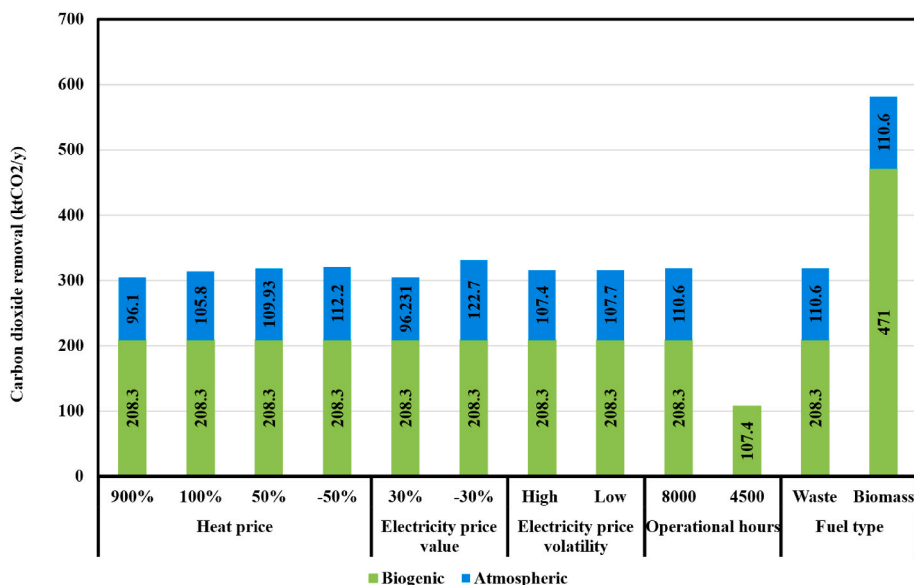


Fig. 8. The sensitivity of the annual CDR to variations in five key parameters for the CHP-PCC-DAC system. Data tags for each column represent the respective change of the sensitivity parameter given in each section.

similar levels of fuel consumption in most of the sensitivity cases. Therefore, similar levels of biogenic CDR (208.3ktCO<sub>2</sub>/y), while the maximum possible amount of atmospheric CO<sub>2</sub> removal, according to the optimization results, is 122.7 ktCO<sub>2</sub>/y, which is attained in the case with the low electricity price.

As the price of heat increases, the amount of atmospheric CDR declines, although more heat is recovered from the PCC unit via the LTHP. This indicates that the supply of heat recovered via LTHP to DH for sales is prioritized over upgrading the LTHP heat via the HTHP, with subsequent use in s-DAC for carbon removal. At 100 % higher heat prices, the system will choose to install LTHP if electricity prices are <150 €/MWh. The heat produced by the LTHP will be supplied directly to DH unless heat from the LTHP is required for full-load operation of s-DAC. At 900 % higher heat price, - representative for load-following plants in Sweden - larger LTHP capacity would be installed. However, the heat from LTHP in that case would only be supplied to the district heating system to exploit the higher profit margins and thus would not be upgraded for further use in the s-DAC unit.

The results also show that lower electricity prices increase the cost-optimal amount of total CDR. This is due to the reduction in the operational cost of the s-DAC system and the HTHP, which provides more heat for s-DAC, thereby increasing the NCF. On the other hand, although the optimum amount of atmospheric CDR does not show any changes in volatility of electricity prices, a higher capacity of s-DAC will be installed than in cases with lower electricity price volatility. This indicates that at higher electricity price volatility, the system installs a higher s-DAC capacity but operates it for fewer hours, and vice versa.

Furthermore, with fewer operational hours (4500 h/y), investing in s-DAC becomes uneconomical (at a CDR credit of 615 €/tCO<sub>2</sub>). For this reason, CHP plants operating in an intermediate-load role would require higher CO<sub>2</sub> prices to ensure that the s-DAC integration proposed in this work is economically feasible. The number of operational hours appears to have the highest impact on if the DAC integration to CHP plants will be economically feasible or not. Note that although the CDR potential of the CHP-PCC-DAC system is constrained by the number of DH demand hours, it is crucial for the CHP-PCC-DAC system to be profitable. Therefore, the modeling shows that integration of DAC in the CHP plant will be economically feasible for a very large range of price development as long as the plant stay operational during a larger share of the year. Considering the sensitivity results on operational hours and heat price development, such integration would be more suitable for base load plant than for a load following plants.

The biomass-fired CHP plant considered in this work has a lower heat efficiency than the waste-fired CHP plant considered (see Table 2), and this leads to lower amounts of heat being available for the s-DAC system. However, the change in atmospheric CDR is negligible, and almost equal to that of the waste-fired CHP plant. On the other hand, as the fuel changes from waste to biomass there is a substantial increase in the total amount of CDR achieved (captured from the flue gas) due to the higher biogenic content of biomass compared to waste.

Another key parameter affecting the optimal s-DAC capacity is its specific investment cost, which—together with electricity and CDR credit prices—determines the NCF of the integrated DAC unit. The minimum CDR price at which the model chooses to install s-DAC with low capacity is determined for two cases: i) a minimum projected investment cost for s-DAC at 8 M€/tCO<sub>2</sub> installed capacity; and ii) a maximum predicted investment cost for s-DAC at 70 M€/tCO<sub>2</sub> installed capacity. For a specific investment cost of 8 M€/tCO<sub>2</sub> installed capacity, s-DAC starts to appear in the optimal solution at a CDR credit price of 215 €/tCO<sub>2</sub>. The corresponding value when considering investment cost estimations of 70 M€/tCO<sub>2</sub> installed capacity is 940 €/tCO<sub>2</sub>.

The base case optimization shows that atmospheric CDR corresponds to 82 kg CO<sub>2</sub> per MWh of fuel combusted. At a CDR credit price of 615 €/tCO<sub>2</sub>, this would be equivalent to 50.4€/MWh of heat generated by the boiler for CDR credit generated via s-DAC. The corresponding values for heat and electricity are 5 €/MWh and 55.8 €/MWh, respectively, for the

base case. This would make atmospheric CDR the intermediate product from the NCF point of view. However, including biogenic CDR increases the value to 145 €/MWh (equivalent to 237 kg CO<sub>2</sub> per MWh of fuel combusted), which makes CDR the most revenue generating product of the plant. Given the full freedom of plant operation, the plant would thus only operate for CDR.

In countries such as Sweden, where CHP plants delivering DH play a major role in the energy system, this scheme can be significant in terms of achieving the national target for CDR. Thus, considering the average 82 kg of carbon removal per MWh of fuel combusted, approximately 3.3 Mt of CDR can be achieved annually via s-DAC from the CHP-PCC-DAC system if s-DAC is retrofitted to existing CHP plants with thermal capacities above 50 MWth in Sweden. Of course, this implies a reduction in the amount of heat supplied to the DH networks, which needs to be compensated, either by reduced heat demands through energy efficiency measures in the building stock or by increasing the supply from other heat sources, such as industrial waste heat, electrical boilers and heat pumps.

#### 4.4. Limitations

Four main limitations in the present work should be mentioned: i) the model is based solely on the closure of energy balances, assuming that mass balances, i.e. mass flows, can be adjusted accordingly to satisfy the energy balances, ii) the temperature levels of the DH and DAC systems are assumed to remain constant throughout the year, iii) the efficiency of the CHP plant is assumed to remain constant across different load levels, and iv) the techno-economic analysis is carried out assuming that the CHP plant would remain operational over the lifetime of new equipment installations. It should be noted that although the DAC unit can operate standalone, it will also require to use electricity from grid with a certain carbon footprint, rather than carbon neutral energy supply from the CHP-PCC plant, i.e. this reduces the carbon removal efficiency of the DAC.

Future research should aim to develop a more detailed representation of the integrated system, incorporating mass balance considerations and accounting for the time-varying operation of the CHP, PCC and DAC processes throughout the year. This would enable a refined study of the integration concept presented in this work. Future research can also move towards using the presented framework for assessing the scale of possible DAC integration at industrial sites where waste heat is available for s-DAC operation.

## 5. Conclusions

A scheme for the integration of s-DAC into CHP plants equipped with post-combustion capture is proposed (CHP-PCC-DAC), using a Swedish 167-MWth CHP plant as reference. The scheme provides DH plants with the opportunity to increase the plant's total capture and, depending on the value of CDR credit prices, it offers increased NCF from providing CDR, as well as progression towards meeting climate goals.

For the reference plant, it is found that the CHP-PCC-DAC scheme is economically feasible under the different scenarios considered in the sensitivity analysis for CDR credit prices in the range of 279–685 €/tCO<sub>2</sub>. Values in this range are notably lower than current CDR credit prices in the voluntary market (>1000 €/tCO<sub>2</sub>). These values were calculated by assuming conservative values for the electricity price and specific investment costs for low-temperature and high-temperature heat pumps, PCC, and s-DAC units. Therefore, it can be concluded that CHP plants connected to a DH network are suitable locations for installing s-DAC, as an alternative to locating s-DAC next to storage sites. Entering the new market for CDR credits, which could constitute a large share of the plant's NCF based on the CDR credit price, would allow for enhanced exploitation of the existing CHP infrastructure and provide opportunities for new operational strategies for the CHP plant, which are currently constrained by the seasonal variations of the DH demand.

The results from the optimization model reveal that the operational parameters that will most strongly favor atmospheric CDR in the proposed system are lower electricity prices and a higher number of operational hours for the plant. In contrast, the installed capacity and total atmospheric CDR of the proposed scheme are less sensitive to fuel type, electricity price volatility, and heat price. Furthermore, the capital cost of s-DAC would be directly related to the installed capacity of s-DAC in the optimal solution. The results also highlight the potential for achieving high levels of CDR through retrofit of existing large-scale CHP plants connected to district heating networks, which would facilitate the achievement of CDR targets.

#### CRedit authorship contribution statement

**Sina Hoseinpoori:** Writing – review & editing, Writing – original draft, Visualization, Methodology, Formal analysis, Data curation, Conceptualization. **Tharun Roshan Kumar:** Writing – review & editing, Writing – original draft, Methodology, Conceptualization. **Johanna Beiron:** Writing – review & editing, Supervision, Methodology. **Filip Johnsson:** Writing – review & editing, Funding acquisition. **Elin Svensson:** Writing – review & editing. **David Pallarès:** Writing – review & editing, Supervision, Methodology.

#### Declaration of generative AI and AI-assisted technologies in the writing process

During the preparation of this work, the author(s) used ChatGPT in order to improve the language and readability. After using this tool/service, the authors reviewed and edited the content as needed and take (s) full responsibility for the content of the publication.

#### Declaration of competing interest

The authors declare that they have no known competing financial interests or personal relationships that could have appeared to influence the work reported in this paper.

#### Acknowledgments

The authors acknowledge financial support from the Swedish Energy Agency and project partners within the project “Negative Emissions with Direct Air Capture for Sweden” (P 2020–008294).

#### Nomenclature

##### Abbreviations

ACLC	Actual cooling load curves
ANF	Annualization factor
bio-CCS	Biomass combustion with carbon capture and storage
BS	Share of biogenic carbon in fuel
Cap	Capacity of the plant
CAPEX	Capital expenditure
CC	Carbon content
CCS	Carbon capture and storage
CDR	Carbon dioxide removal
CHP	Combined heat and power
CHP-PCC	Combined heat and power plant equipped with CCS
CHP-PCC-DAC	Combined heat and power plant equipped with post-combustion capture and integrated with direct air capture
COP	Coefficient of performance
CR	Capture rate
DAC	Direct air capture
DH	District heating
EU-ETS	European Union Emissions Trading System
FGC	Flue gas condenser
HHV	Higher heating value

HTHP	High-temperature heat pump
LP	Linear programming
LHV	Lower heating value
LTHP	Low-temperature heat pump
MEA	Monoethanolamine
NGCC	Natural gas combined cycle
NCF	Net cash flow
NPV	Net present value
PCC	Post-combustion capture
s-DAC	Solid sorbent direct air capture

##### Symbols

C	Cost/price (€)
$C_i^{inv}$	investment cost in technology $i$ (€)
CP	Specific heat capacity (J/Kg.K)
h	hour
$\dot{m}$	mass flow (t/h)
M	molecular weight (kg/kmol)
P	power (MW)
Q	heat (MW)
s	installed capacity (MW)
T	temperature (K)
t	time (year)
$\Delta$	difference

##### Subscripts and superscripts

B	boiler
c	Carbon
Carnot	carnot
C&L	Compression and liquefaction
CDR	Carbon dioxide removal
Cond	Condenser
dem	Demand
Evap	Evaporator
FGC	Flue gas condenser
Fossil	emissions with fossil origins
Fuel	Fuel
gen	Total generated
HX	Heat exchanger
HP	Heat pump
i	Technology in the set of technologies I
in	Inlet
inv	Investment
Lift	Lift temperature in HP
Mid	Middle level temperature
min	Minimum
neg	Negative emissions
net	net
Out	Outlet
Sink	Heat sink in HP
Sorbent	solid sorbent
Supply	supply
Target	target
Tot	Total
WF	working fluid

##### Greek letters

$\eta$	efficiency (%)
--------	----------------

#### Data availability

Data will be made available on request.

## References

- [1] IPCC. Mitigation of climate change climate change 2022 working group III contribution to the sixth assessment report of the intergovernmental panel on climate change. 2022.
- [2] 2050 long-term strategy. 2050 long-term strategy - european commission [Online]. Available: [https://climate.ec.europa.eu/eu-action/climate-strategies-targets/2050-long-term-strategy\\_en](https://climate.ec.europa.eu/eu-action/climate-strategies-targets/2050-long-term-strategy_en). [Accessed 7 October 2024].
- [3] Sweden's climate goals. Sweden's climate goals - krisinformation.se [Online]. Available: <https://www.krisinformation.se/en/hazards-and-risks/climate-change/swedens-climate-goals>. [Accessed 7 October 2024].
- [4] och Regeringskansliet R. Vägen till en klimatpositiv framtid [Online]. Available: <https://www.regeringen.se/rattsliga-dokument/statens-offentliga-utredningar/2020/01/sou-20204/>. [Accessed 7 October 2024].
- [5] IEA. Direct air capture: a key technology for net zero. 2022.
- [6] Beiron J, Montañés RM, Normann F, Johnsson F. Combined heat and power operational modes for increased product flexibility in a waste incineration plant. *Energy Jul. 2020*;202:117696. <https://doi.org/10.1016/J.ENERGY.2020.117696>.
- [7] Beiron J, Normann F, Johnsson F. A techno-economic assessment of CO2 capture in biomass and waste-fired combined heat and power plants – a Swedish case study. *Int J Greenh Gas Control Jul. 2022*;118:103684. <https://doi.org/10.1016/J.IJGGC.2022.103684>.
- [8] Deutz S, Bardow A. Life-cycle assessment of an industrial direct air capture process based on temperature–vacuum swing adsorption. *Nat Energy Feb. 2021*;6(2):203–13. <https://doi.org/10.1038/s41560-020-00771-9>.
- [9] T. Terlouw, K. Treyer, C. Bauer, and M. Mazzotti, "Life cycle assessment of direct air carbon capture and storage with low-carbon energy sources supplementary information (SI)." [Online]. Available: [https://www.engineeringtoolbox.com/met-al-alloys-densities-d\\_50.html](https://www.engineeringtoolbox.com/met-al-alloys-densities-d_50.html).
- [10] Tanzer SE, Ramfrez A. When are negative emissions negative emissions? *Energy Environ Sci Apr. 2019*;12(4):1210–8. <https://doi.org/10.1039/C8EE03338B>.
- [11] Drechsler C, Agar DW. Characteristics of DAC operation within integrated PtG concepts. *Int J Greenh Gas Control Feb. 2021*;105:103230. <https://doi.org/10.1016/J.IJGGC.2020.103230>.
- [12] Jeong-Potter C, Farrauto R. Feasibility study of combining direct air capture of CO2 and methanation at isothermal conditions with dual function materials. *Appl Catal, B Mar. 2021*;282:119416. <https://doi.org/10.1016/J.APACATB.2020.119416>.
- [13] Schäppi R, et al. Drop-in fuels from sunlight and air. *Nature 2021 Nov. 2021*;601(7891):63–8. <https://doi.org/10.1038/s41586-021-04174-y>. 601:7891.
- [14] Singh U, Colosi LM. Capture or curtail: the potential and performance of direct air capture powered through excess renewable electricity. *Energy Convers Manag X Aug. 2022*;15:100230. <https://doi.org/10.1016/J.ECMX.2022.100230>.
- [15] Bertoni L, Roussanaly S, Riboldi L, Anantharaman R, Gazzani M. Integrating direct air capture with small modular nuclear reactors: understanding performance, cost, and potential. *J Phys Energy Apr. 2024*;6(2). <https://doi.org/10.1088/2515-7655/AD2374>.
- [16] Wiegner JF, Grimm A, Weimann L, Gazzani M. Optimal design and operation of solid sorbent direct air capture processes at varying ambient conditions. *Ind Eng Chem Res Aug. 2022*;61(34):12649–67. <https://doi.org/10.1021/ACS.IECR.2C00681>.
- [17] Leonzio G, Shah N. Innovative process integrating air source heat pumps and direct air capture processes. *Ind Eng Chem Res Sep. 2022*;61(35):13221–30. [https://doi.org/10.1021/ACS.IECR.2C01816/ASSET/IMAGES/LARGE/IE2C01816\\_0007.JPEG](https://doi.org/10.1021/ACS.IECR.2C01816/ASSET/IMAGES/LARGE/IE2C01816_0007.JPEG).
- [18] Sagues WJ, Park S, Jameel H, Sanchez DL. Enhanced carbon dioxide removal from coupled direct air capture–bioenergy systems. *Sustain Energy Fuels Oct. 2019*;3(11):3135–46. <https://doi.org/10.1039/C9SE00384C>.
- [19] Okonkwo EC, AlNouss A, Shahbaz M, Al-Ansari T. Developing integrated direct air capture and bioenergy with carbon capture and storage systems: progress towards 2 °C and 1.5 °C climate goals. *Energy Convers Manag Nov. 2023*;296:117687. <https://doi.org/10.1016/J.ENCONMAN.2023.117687>.
- [20] Cheng P, et al. Modeling and optimization of carbon-negative NGCC plant enabled by modular direct air capture. *Appl Energy Jul. 2023*;341:121076. <https://doi.org/10.1016/J.APENERGY.2023.121076>.
- [21] Climeworks switches on world's largest direct air capture plant." Accessed: November. 6, 2024. [Online]. Available: <https://climeworks.com/press-release/climeworks-switches-on-worlds-largest-direct-air-capture-plant-mammoth>.
- [22] Levihn F. CHP and heat pumps to balance renewable power production: lessons from the district heating network in Stockholm. *Energy Oct. 2017*;137:670–8. <https://doi.org/10.1016/J.ENERGY.2017.01.118>.
- [23] Roshan Kumar T, Beiron J, Biermann M, Harvey S, Thunman H. Plant and system-level performance of combined heat and power plants equipped with different carbon capture technologies. *Appl Energy May 2023*;338:120927. <https://doi.org/10.1016/J.APENERGY.2023.120927>.
- [24] District heating - Energimarknadsinspektionen." Accessed: October. 7, 2024. [Online]. Available: <https://www.ei.se/ei-in-english/district-heating>.
- [25] Young J, et al. The cost of direct air capture and storage: the impact of technological learning, regional diversity, and policy. *Chem Jun. 2022*. <https://doi.org/10.26434/CHEMRXIV-2022-DP36T>.
- [26] Sievert K, Schmidt TS, Steffen B. Considering technology characteristics to project future costs of direct air capture. *Joule Apr. 2024*;8(4):979–99. <https://doi.org/10.1016/J.JOULE.2024.02.005>.
- [27] Sendi M, Bui M, Mac Dowell N, Fennell P. Geospatial analysis of regional climate impacts to accelerate cost-efficient direct air capture deployment. *One Earth Oct. 2022*;5(10):1153–64. <https://doi.org/10.1016/J.ONEEAR.2022.09.003>.
- [28] S. Karlsson, "Energy infrastructures for low-carbon-emitting industries," 2024, Accessed: November. 8, 2024. [Online]. Available: <https://research.chalmers.se/en/publication/543174>.
- [29] Mühlbauer A, Keiner D, Breyer C. Techno-economic insights and deployment prospects of permanent carbon dioxide sequestration in solid carbonates. *Energy Environ Sci Nov. 2024*;17(22):8756–75. <https://doi.org/10.1039/D4EE03166K>.
- [30] Biermann M, Normann F, Johnsson F, Skagestad R. Partial carbon capture by absorption cycle for reduced specific capture cost. *Ind Eng Chem Res Nov. 2018*;57(45):15411–22. <https://doi.org/10.1021/acs.iecr.8b02074>.
- [31] Young J, McIlwaine F, Smit B, Garcia S, van der Spek M. Process-informed adsorbent design guidelines for direct air capture, vol. 456; 2023. <https://doi.org/10.1016/j.cej.2022.141035>.
- [32] Deng H, Roussanaly S, Skaugen G. Techno-economic analyses of CO2 liquefaction: impact of product pressure and impurities. *Int J Refrig Jul. 2019*;103:301–15. <https://doi.org/10.1016/J.IJREFRIG.2019.04.011>.
- [33] Roshan Kumar T, Beiron J, Biermann M, Harvey S, Thunman H. Plant and system-level performance of combined heat and power plants equipped with different carbon capture technologies. *Appl Energy 2023*;338(Febuary):120927. <https://doi.org/10.1016/j.apenergy.2023.120927>.
- [34] Beiron J, Johnsson F. Progressing from first-of-a-kind to Nth-of-a-kind: applying learning rates to carbon capture deployment in Sweden. *Int J Greenh Gas Control Sep. 2024*;137:104226. <https://doi.org/10.1016/J.IJGGC.2024.104226>.
- [35] Thunman H, et al. Circular use of plastics-transformation of existing petrochemical clusters into thermochemical recycling plants with 100% plastics recovery. *Sustain Mater Technol Dec. 2019*;22. <https://doi.org/10.1016/j.susmat.2019.e00124>.
- [36] Phyllis2 - ECN Phyllis classification." Accessed: December. 6, 2024. [Online]. Available: <https://phyllis.nl/Browse/Standard/ECN-Phyllis#wood%20chi%C3%A5>.
- [37] Maciejowska K. Assessing the impact of renewable energy sources on the electricity price level and variability – a quantile regression approach. *Energy Econ Jan. 2020*;85:104532. <https://doi.org/10.1016/J.ENERG.2019.104532>.
- [38] Simon Öberg, Lisa Göransson, Hanna Ek Fälthb, Uli Rahmlowc, and Filip Johnsson, "Evaluation of hydropower equivalents in energy systems modeling.".
- [39] S. Akerfeldt, M.-O. Hansson, and D. Waluszewski, "Sweden's carbon tax," Government Offices of Sweden. Accessed: June. 1, 2024. [Online]. Available: <https://www.government.se/government-policy/swedens-carbon-tax/swedens-carbon-tax/#:~:text=Swedishcarbontaxrates&text=Thecarbontaxwasintroduced,ofSEK10.87perEUR>.
- [40] Young J, et al. The cost of direct air capture and storage can be reduced via strategic deployment but is unlikely to fall below stated cost targets. 2023. <https://doi.org/10.1016/j.oneear.2023.06.004>.